GEOPHYSICS, VOL. 68, NO. 3 (MAY-JUNE 2003); P. 815–823, 12 FIGS., 2 TABLES.
10.1190/1.1581034

Case History

Time-lapse tomography

Aldo L. Vesnaver*, Flavio Accaino‡, Gualtiero Bohm‡, Gianni Madrussani‡, Jan Pajchel**, Giuliana Rossi‡, and Giancarlo Dal Moro§

ABSTRACT

In time-lapse analysis, we have to distinguish the seismic response changes due to oil and gas production at a reservoir over the years from several other causes, such as the recording signature and random noise. In this paper, we focus our attention on the velocity macromodel provided by seismic tomography, which is a basic tool for the data regularization, its depth or time migration, and a possible final subtraction among different vintages. We show first that we cannot use just a single velocity model for all data sets, because of seasonal variations of the overburden velocity (which is mainly due to seawater temperature in marine cases and to the water table depth in land cases). However, we can exploit the basic assumption of time-lapse analysis for constraining reflection/refraction tomography, i.e., by imposing the constraint that the layer structure and the local velocities do not change outside the reservoir (and in the shallowest part) over time. We thus get coupled models that are physically consistent, with a better spatial coverage and higher information redundancy. The new method is illustrated by a marine case history from the North Sea.

INTRODUCTION

Time-lapse analysis relies on a simple basic principle: if the seismic response changes in time due only to oil and gas production from a reservoir, we can exploit these variations to detect fluid movements and optimize the production. This principle assumes implicitly that seismic experiments are repeatable or, at least, are so in all earth domains outside the reservoir. Only in this case, in fact, seismic response variations may have a diagnostic value.

Although several successful case histories were reported in the last decade (see, e.g., Johnstad et al., 1995; Watts et al., 1996; Sønnenland et al., 1997; Ebrom et al. 1998; Landrø et al., 1999; Rached and Marschall, 1999; Johnston et al., 2000; Davis and Benson, 2001), several problems remain in time-lapse analysis, mostly related to approximating the hypotheses mentioned above. First, we know that random noise contaminates our signal; in some cases, the expected time-lapse variations may be lower than the noise level. Secondly, especially at sea, it is hard repeating a previous recording geometry identically; thus, some accurate interpolation algorithm must be adopted that is able to fully honor the wave equation. Third, even if a perfect interpolation algorithm is available, we must rely on a very precise navigation or topographic survey for getting an adequate input to it. The possible alternative of deploying permanent instruments puts other problems, such as fishing activity, curious people, deterioration of the permanent receivers, and no guarantee that their earth coupling and instrumental efficiency is unchanged after, let us say, ten years. Thus, we must compensate (in a surface consistent manner) for the possible variations of source and receiver coupling and directivity; often, they change from legacy data to data collected by current technologies. Finally, especially at wells, some leakage of gas into the overburden or a subsidence phenomenon may change further the seismic response in time.

In addition to the main physical aspects, there are further aspects in the data processing. After the compensations listed above, we must adopt an identical processing sequence for the different data vintages. Since processing codes also evolve in

Published on Geophysics Online February 10, 2003. Manuscript received by the Editor December 3, 2001; revised manuscript received December 31, 2002.
*Formerly OGS, Borgo Grotta Gigante 42/c, 34010 Trieste, Italy; presently Saudi Aramco, Post Office Box 12668, Dhahran 31311, Saudi Arabia. E-mail: aldo.vesnaver@aramco.com.
‡OGS, Borgo Grotta Gigante 42/c, 34010 Trieste, Italy. E-mail: faccaino@ogs.trieste.it; gbohm@ogs.trieste.it; gmadrussani@ogs.trieste.it; grossi@ogs.trieste.it.
**Norsk Hydro, Sandsliveien 90, 5020 Bergen, Norway. E-mail: jan.pajchel@nho.hydro.com.
§Formerly OGS, Borgo Grotta Gigante 42/c, 34010 Trieste, Italy; presently University of Trieste, Exploration Geophysics Group, Department of Geological Environmental and Marine Sciences, Via Weiss 1, 34127 Trieste, Italy. E-mail: dalmoro@units.it.

time, we can expect, for example, that the same deconvolution parameters could provide a bit different output in the latest software release than is one available five years ago. It is quite normal that some algorithm simplification or code speedup has been pursued, plus some bug removal (or addition). Thus, complete reprocessing of all available data vintages is a good practice.

All these difficulties are part of recent and current research, development, and testing (see, e.g., Nur, 1989; Lumley et al., 1994; Ross et al., 1996; Davis et al., 1997; Rickett and Lumley, 1998; Sønneland et al., 1998; Landrø, 1999, 2001; Marschall, 1999; Ronen et al., 1999; Tura and Lumley, 1999; Reid and MacBeth, 2000; Majer et al., 2001; Stucchi et al., 2001; Vesnaver et al., 2001). In this paper, we study a further problem for time-lapse analysis: the seasonal variations of the overburden (the seawater layer in marine surveys, the water table on land). Their effect, when not compensated for, can totally hide the sought time-lapse variations. We introduce a tool for overcoming this drawback and making the tomographic models more robust, which we call "time-lapse tomography." In this approach, we get a set of coupled depth models, which are the basic input for the possible prestack depth migration of the different vintages. Thus, if all other problems mentioned above are solved by a crosscalibration, we can subtract properly the different data volumes and highlight the reservoir changes.

THE UPPERMOST LAYER

In both land and marine cases, seasons can significantly change the seismic velocities in the uppermost layer. On land, the water table depth depends heavilly on the rain rate; at sea, the water temperature is affected by sun radiation and seasonal winds. Winds also produce sea-surface waves, which introduce time-variant static shifts and increase the noise level. These effects must be compensated for in time-lapse analysis.

Several empirical relationships are available in the oceanographic literature relating sound speed in seawater to physical parameters. For example, Mackenzie (1981) expressed the velocity v as a function of temperature T (°C), water depth z (m), and salinity s (psu) as

$$v(T,s,z) = \eta + \chi T + \delta T^2 + \varphi T^3 + \sigma(s-35.0) + \mu z + \gamma z^2 + \alpha T z^3 + \beta T(s-35.0), \quad (1)$$

where Greek letters indicate empirical constants. Their values are listed in Table 1.

Temperature is the dominating factor in most cases, and is related to sea currents and seasons. Salinity changes locally very little and changes slowly during the years as a function of the global circulation and climate, except in some areas near rivers. The water depth affects the local velocity weakly through the increasing pressure of the overlying water. A much more relevant related effect is the decreasing influence as a function of depth of surface heating and cooling from the sun and wind. Generally, the uppermost water layer (called the thermocline) has a thickness of a few to 100 m, whether in shallow seas or in the ocean. Below it, the water temperature (and thus the sound speed) remains quite constant in time. Figure 1 shows the daily change of shallow seawater temperature during 1996 in areas adjacent to Gullfaks (Martin Landrø, personal communication, 2002). We notice a seasonal change

Table 1. Numerical values of the empirical constants in the Mackenzie (1981) formula, which relates the sound speed in seawater to salinity, depth, and temperature.

Parameter	Empirical value
η	1448.96
χ	4.591
δ	-5.304×10^{-2}
φ	2.374×10^{-4}
σ	1.340
μ	1.630×10^{-2}
γ	1.675×10^{-7}
α	-7.139×10^{-13}
β	-1.025×10^{-2}

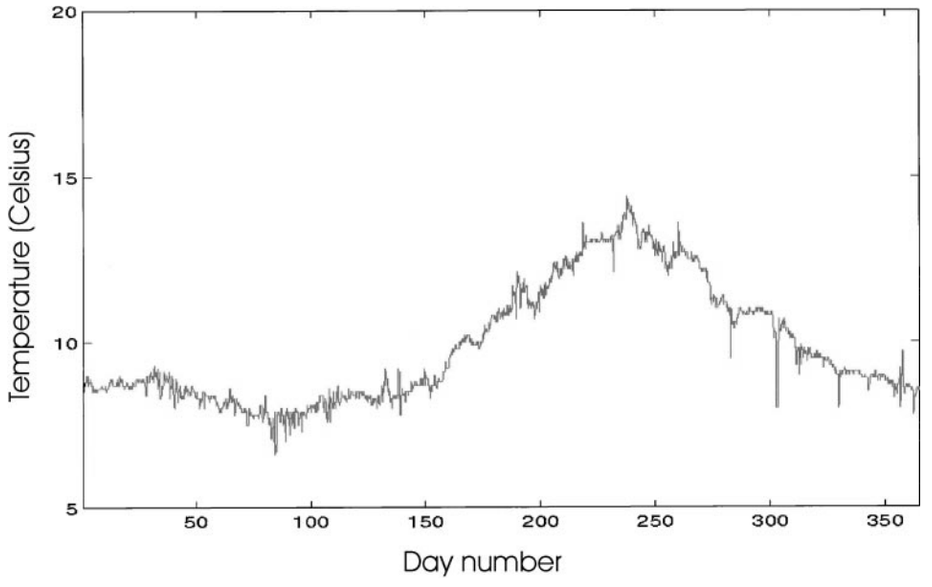

FIG. 1. Temperature variations of seawater in the Gullfaks area of the North Sea during 1996 (courtesy of Martin Landrø).

of 5°C, but the peak difference reaches 8°C. Figure 2 displays a general temperature trend as a function of depth for the Atlantic Ocean (see, e.g., Chiu et al., 1996).

Using the Mackenzie (1981) formula, one can see that a temperature change of 5°C, which is not rare over a year, causes a velocity change Δv exceeding 22 m/s in the seawater sound speed i.e., larger than 1.5%. By neglecting this change, we introduce a systematic error in the traveltime inversion. For a reflector depth z, the normal moveout difference ΔNMO due to a deviation Δv from the correct velocity v_{OK} may be expressed as a function of the traveltimes t_0 and t_x, respectively, at offsets zero and x:

$$\begin{aligned}\Delta NMO &= \frac{x^2}{2t_0}\left(\frac{1}{v_{OK}^2} - \frac{1}{(v_{OK}+\Delta v)^2}\right)\\ &= (t_x - t_0)\left[1 - \left(\frac{v_{OK}}{v_{OK}+\Delta v}\right)^2\right]\\ &= \frac{x^2 v_{OK}}{4z}\left(\frac{1}{v_{OK}^2} - \frac{1}{(v_{OK}+\Delta v)^2}\right). \qquad (2)\end{aligned}$$

For example, for a sea floor depth of 100 m and an offset exceeding about 2000 m, the traveltime error is larger than 200 ms! If we are matching common-offset sections of different data vintages, or just depth-migrating those from a single survey, we will sum out-of-phase the signals from the sea floor and compromise all later arrivals. Sometimes, one tries to compensate for this error by applying "static" corrections to the marine data, but this implies neglecting ray bending and choosing to focus either on the shallower layers or on some deeper target.

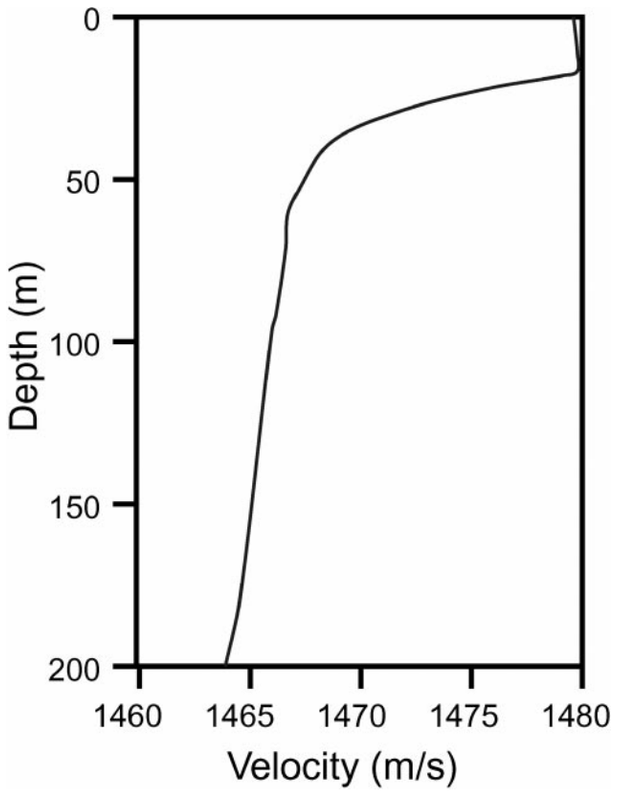

FIG. 2. A typical curve of sea water velocity as a function of depth in the Atlantic Ocean.

Static corrections are appropriate, on the other hand, for cable depth and tidal variations. Tidal variations frequently reach 2 m in this area of the North Sea.

For the land case, the velocity change in the weathered domains above and below the water table may be much larger. For example, for a velocity step of 2 km/s, the two-way vertical traveltime varies by 1 ms for each meter of water table shift. Seasonal variations of several meters are common and thus, especially at large offsets, we can expect travel time changes of a similar order of magnitude as in the marine case. If we impose the condition that the static corrections are the same (e.g., because we deployed permanent geophones), the direct subtraction of corresponding traces among different vintages will be degraded.

We can draw here a first conclusion: time-lapse changes in the uppermost layer are comparable to those ones we are seeking at the reservoir level. Uncompensated seasonal effects can create spurious time-lapse phenomena, or just hide the deepest ones. In the next section, we check this theory by a case history from the North Sea.

A NORTH SEA CASE HISTORY

Oseberg field was discovered in the 1980s, with oil and gas production beginning in 1989. Two 3D surveys were carried out in 1989 and 1992, whose main features are reported in Table 2; further details are in Johnstad et al. (1995). In 1989, a vessel towing just two streamers with a central source was used; in 1992, one vessel carried three streamers and the source, while a second vessel towed two additional streamers. Despite a few similarities, the recording geometry is quite different in the two vintages. These differences are larger when looking at the shot point locations (Figure 3), and even more when considering the rapidly varying feathering effect caused by currents and navigation obstacles (Figure 4). These differences make a direct comparison of seismic profiles in the time domain difficult, and require at least an accurate interpolation and regularization into a common reference. The strategy we adopted was building a 3D depth model by reflection and refraction tomography, and then depth-migrating the data sets for a geometry-independent comparison.

First, we picked and separately inverted the traveltimes of the two data vintages. Figures 5 and 6 allow comparing, respectively, vertical and horizontal slices of the 1989 and 1992 tomographic macromodels, obtained by estimating independently

Table 2. Main recording parameters for the 1989 and 1992 surveys.

	December 1989–January 1990	April–July 1992
Source type	Air gun (2400 in^3)	Sleeve gun (3400 in^3)
Vessels	1	2
Streamers	2	5
Streamer interval	100 m	75 m
Source offset	80 m	120 m
Source depth	6 m	6 m
Streamer length	2987.5 m	2987.5 m
Receiver interval	25 m	12.5 m
Receiver depth	5 m	7 m
Shot interval	25 m	25 m
Sampling rate	2 ms	2 ms
Channels	480	1200

both the velocity and the main interfaces' structure in three dimensions. The sea-floor depth practically coincides in the two models, the same similarity occurs everywhere. In the lower layers (Figure 5), the differences are a bit larger and increase with depth, but rarely exceed 12 m. We notice quite large variations in the local velocities, both where we expect them (uppermost layer and the target, shown by the arrow) and also elsewhere (where no time-lapse effect should occur). However, we notice a significant velocity decrease at the target zone, indicated by an arrow. Particularly impressive is the consistent regional trend of seawater local variations (Figure 6). In a few areas, the estimated velocity difference at a given location between the 1989 and 1992 surveys reaches 50 m/s (i.e. a value considered unacceptable in the previous section for time-lapse analysis). Part of this difference could be due to positioning errors and streamer feathering; streamer feathering was quite strong in a few profiles, but was mitigated by the 3D inversion approach, which took it into account.

The algorithm we adopted for the tomographic inversion is described in detail by Vesnaver et al. (1999). Here, we briefly recall that the algorithm separately estimates the velocity field and the interface structure to reduce their cross talk. The traveltimes are modeled by a minimum-time ray-tracing algorithm (Vesnaver, 1996; Böhm et al., 1999), able to simulate the kinematics of direct, reflected, refracted, and diffracted waves in irregularly shaped homogeneous voxels. The velocities are estimated by a SIRT approach (see, e.g., van der Sluis and van der Vorst, 1987), followed by a natural smoothing obtained by staggered grids (Vesnaver and Böhm, 2000). The structure depth is obtained by reflected or refracted arrivals, or both. Vesnaver et al. (1999) proved the noticeable contribution of head waves for improving the depth model for prestack depth migration at this site, because it allows reducing the multiples interference and increasing the information redundancy at the shallowest interfaces.

Figure 7 allows comparing the sea-floor image along a line in the 1992 vintage by using both the (improper) 1989 and the (correct) 1992 velocity model. The 1992 model (Figure 7b) is much better imaged not only at the sea floor, but also at a few underlying events. This information is not directly useful for the reservoir monitoring, but it may be important when locating new offshore platforms for oil and gas production. However, when looking at the target area (Figure 8), we notice again that we cannot use the seawater velocity obtained by the 1989 data for the 1992 case. Doing so degrades the image sharpness.

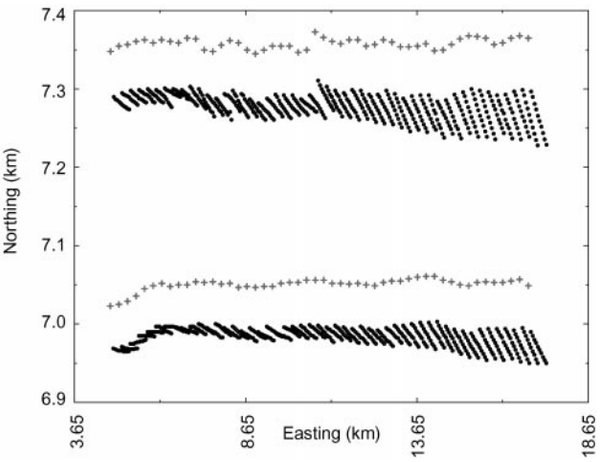

FIG. 4. Feathering effect along a few lines of the 1992 vintage. Crosses depict shot points, dots indicate receiver positions.

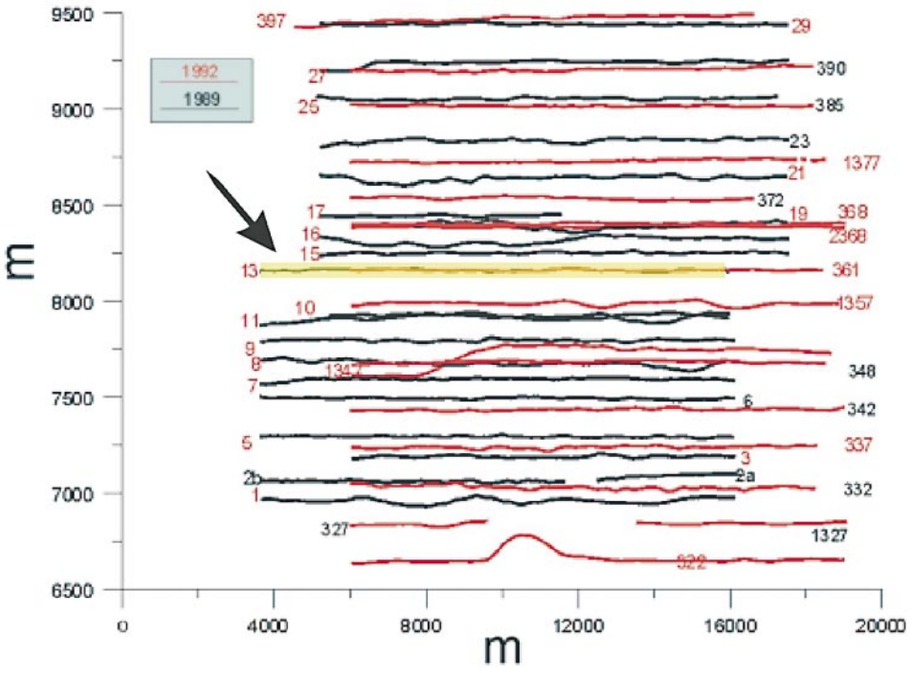

FIG. 3. Shot point map of the 1989 (black lines) and 1992 (red lines) data vintages. The arrow shows a line used for slicing the 3D depth model.

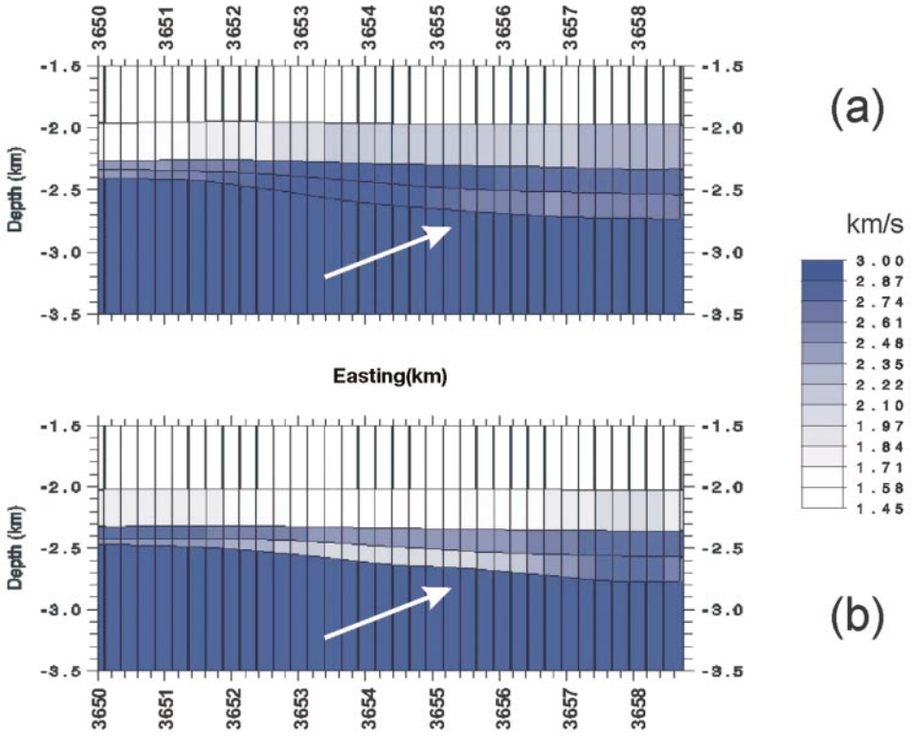

FIG. 5. Vertical section across the 1989 (a) and 1992 (b) tomographic models, obtained by a decoupled inversion, along the line depicted in Figure 3. The arrow indicates the target zone.

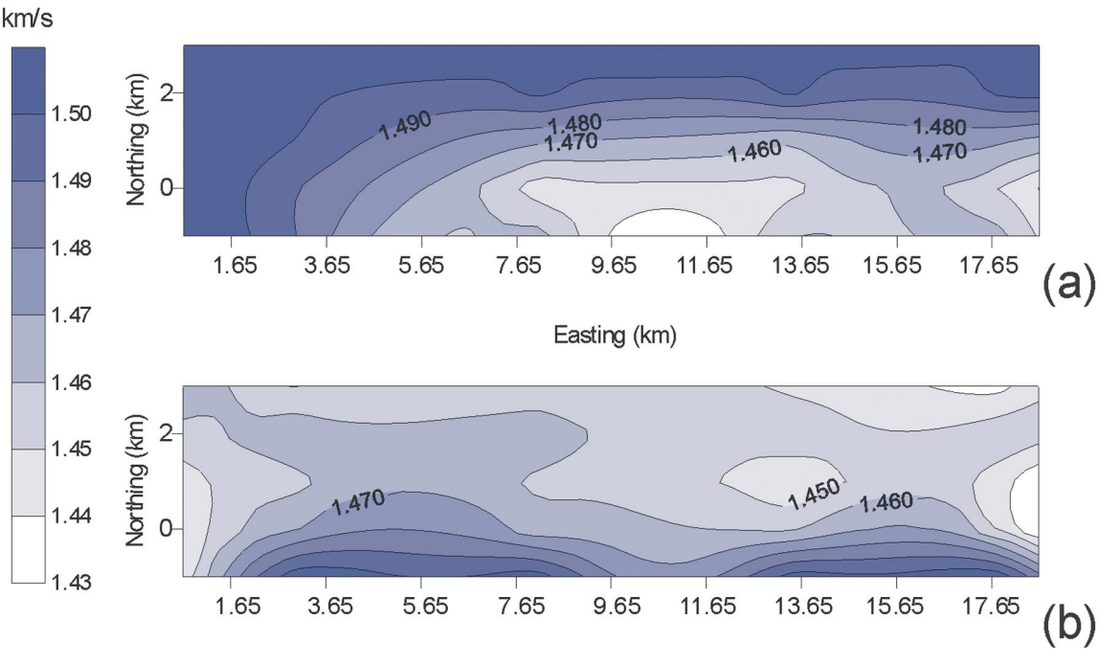

FIG. 6. Horizontal section in the seawater layer across the 1989 (a) and 1992 (b) tomographic models, obtained by a standard decoupled inversion of the 3D surveys.

The near-surface effects are not the only ones that can degrade time-lapse imaging. Possible differences in shot and receiver intervals can reduce the overlap of unaliased spatial frequencies in the migrated vintages, and location changes reduce signal repeatability (see, e.g., Landrø, 1999; Ronen et al., 1999). In the selected profiles, feathering is almost absent, profiles overlap, and the shot interval is the same. The major difference is the receiver interval, which is double in the 1989 vintage.

TIME-LAPSE TOMOGRAPHY

The time invariance of the seismic response is the basic condition for time-lapse analysis, however; such a condition does not hold in both the producing reservoir and the uppermost layer. Thus, when building a macromodel for seismic velocities, we must allow for changes in the estimated velocities there when considering different data vintages; elsewhere, we should impose the condition that velocities are identical. Furthermore, if subsidence phenomena are negligible and we are not inverting for interfaces at the gas/oil/water contacts, we may assume that the whole interface structure is constant in time. These assumptions decide a procedure that we call time-lapse tomography, which can be summarized by the following steps.

1) Pick the traveltimes of the same events among the available seismic vintages.
2) Choose a tomographic grid that is adequate for all vintages.
3) Estimate velocities and interfaces independently for each data vintage, using a common initial model.
4) Average the interface structures into a single one, identical for all vintages.
5) Average the velocity field everywhere, except in the uppermost layer and within the reservoir, so as to a set of coupled models.
6) Compute new traveltimes separately in the partially averaged models, using the proper model for each vintage.

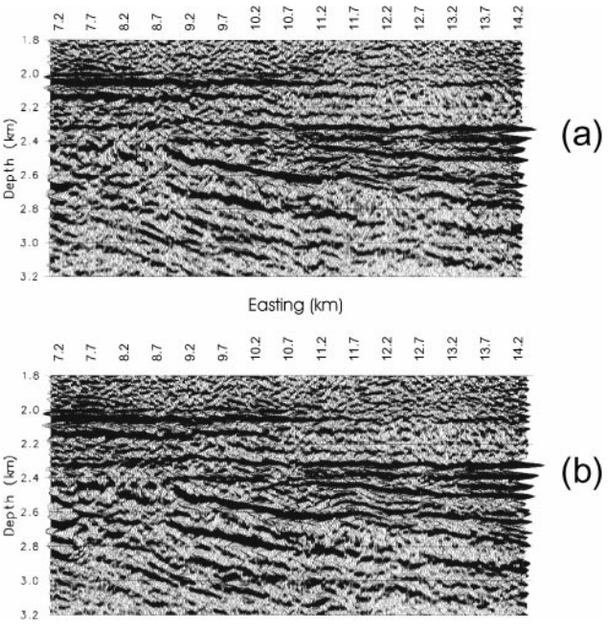

FIG. 8. Prestack depth-migrated images of a line from the 1992 vintage, using the seawater velocity estimated by the 1989 (a) and 1992 (b) data: target zone.

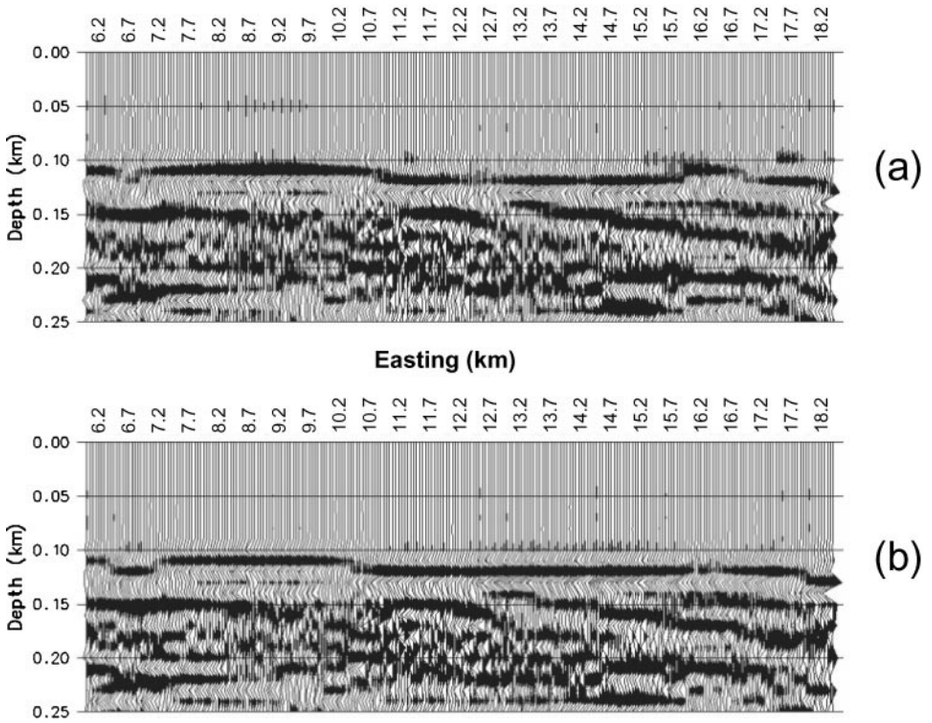

FIG. 7. Prestack depth-migrated images of a line from the 1992 vintage, using the seawater velocity estimated by the 1989 (a) and 1992 (b) data: shallow part.

7) If the match between picked and modeled traveltimes is good, or a maximum iteration number is reached, exit.
8) Update velocities in each model by the new traveltimes for its corresponding vintage.
9) Update interfaces jointly by all new traveltimes (they are the same for all coupled models).
10) If the models' changes are significant somewhere, go back to step 5; otherwise, exit.

Inversion ambiguities may be caused by the null space of the tomographic matrix or by the velocity-depth cross talk. In step 3, using a common initial model for all vintages can reduce false time-lapse effects. Our inversion algorithm does not move the ill-posed parameters from their starting value. Thus, these values would vary falsely if we assume different initial hypotheses for them within each vintage inversion.

Another simple way for getting time-lapse artifacts is choosing a tomographic grid that is well suited for one vintage, but not for all of them. For example, because of recording irregularities (as in Figure 3), some voxels may be void of ray paths for a vintage and well covered for other ones. In the latter cases, the local velocity will likely change with respect to the initial hypothesis, but will not in the void voxels; thus, we would observe an apparent velocity variation. Therefore, step 2 requires particular care. (Unfortunately, even more insidious cases are possible when the null space influence is not properly controlled.)

By applying time-lapse tomography to the 1989 and 1992 vintages, we estimated two coupled models. We chose a coarse grid in the overlap area of these data sets, getting robust, redundant information. In particular, for reducing the recording footprint, we imposed the condition that most voxels are covered by ray paths from different profiles of the same vintage. The different location of sources and receivers among the vintages was an advantage for estimating depth and shape of the model interfaces; thus, we obtained a better depth coverage for the same structure. Finally, we enhanced both resolution and smoothness of the velocity field by staggering the reference grid, while making sure that all voxels are well covered by the different vintages.

Figure 9 shows vertical sections across the same line as in Figure 5. In comparison with the previous decoupled inversion result, note the mostly identical model structure, but a persistent velocity decrease from the 1989 to the 1992 model at the reservoir. This decrease is less pronounced but better focused in the time-lapse (coupled) estimate than the decoupled one in Figure 5. The depth-migrated image obtained by this coupled velocity field (Figure 10a) is sharper than the decoupled one (Figure 10b). Faulted blocks are much clearer, and high-frequency events are now more visible and continuous. A comparable improvement is noticed when comparing the same events in a nearby profile from the 1989 vintage (Figure 11): although the differences are subtle, note again the better quality image (Figure 11b) obtained by time-lapse tomography.

DISCUSSION

By imposing physical constraints and properly exploiting a larger amount of data, time-lapse tomography can reduce some of the ambiguities that can affect the traveltime inversion. Some of them, but not all. Figure 12 shows two sets of common image gathers obtained by prestack depth migrating the same traces from the 1992 vintage, but using the velocities from the

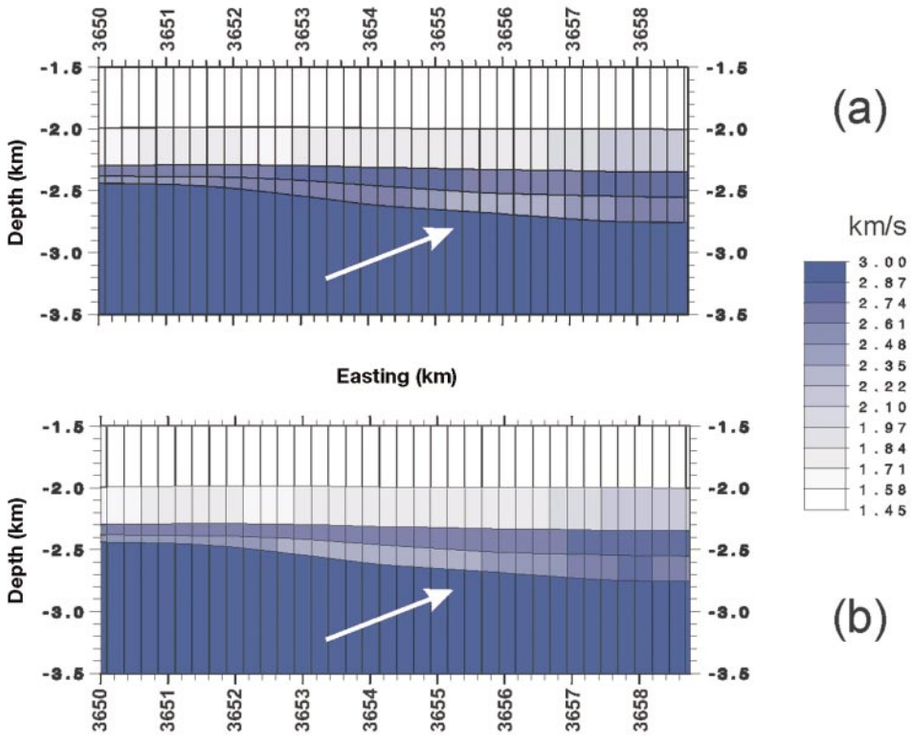

FIG. 9. Vertical section across the 1989 (a) and 1992 (b) tomographic models, obtained by a coupled time-lapse inversion, along the line depicted in Figure 3. The arrow indicates the target zone.

(coupled) 1989 and 1992 tomographic models. The events' flattening is satisfactory in both cases, but the signal quality is quite different. We may notice a higher frequency content when using the 1992 velocity for the 1992 data. Thus, the flattening is a necessary but not sufficient condition for depth imaging, especially for finely tuning these time-varying models.

Time-lapse tomography reduces but does not zero the inversion ambiguities. Therefore, we can still expect both false alarms and signal losses due to different models that perfectly fit the same data or even all available vintages. In same cases, apparent time-lapse variations could be due to different contributions of the null space to the final models; in other cases, the same contributions could mask smaller changes due to real lithologic causes. Further crosschecks are always useful, as is the flatness of common-image gathers; however, even flat common-image gathers do not solve all ambiguities. Figure 12 proves that similar velocities can flatten equally well the main reflections, and that time-lapse effects (such as sea water changes) cannot be estimated according to the flatness principle alone.

CONCLUSIONS

Time-lapse analysis requires an accurate compensation of all known time-varying factors in the seismic traces in order to detect the residual changes due to oil and gas production. Signal crosscalibration and geometry regularization are fundamental tasks, but the velocity macromodel is no less important if our goal is comparing depth-migrated seismic sections and, eventually, their subtraction.

Relevant changes due to seasonal causes occur in the uppermost layer, both in land and marine surveys, which may obscure or degrade those changes sought at the reservoir. We can reduce this drawback by estimating a different depth model for each vintage, but imposing the condition that they must be identical outside the reservoir and below the uppermost layer. These constraints reduce the parameter number and increase the data coverage of the model, in other words, they enhance the robustness and reliability of our estimate.

The flatness principle is a necessary but not sufficient condition for tuning the depth model by checking the common-image gathers in the framework of time-lapse analysis. Additional processing tools and physical criteria should be studied for removing the residual ambiguities, which can degrade the accuracy and reliability of the time-lapse estimates.

ACKNOWLEDGMENTS

This work was partially supported by the European Union in the Thermie Programme (contract n. OG/129/97). We thank

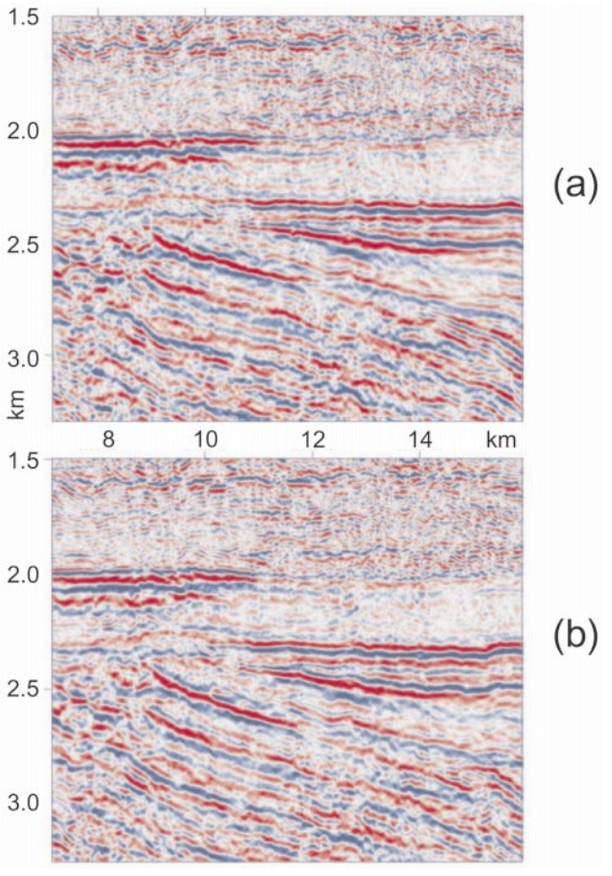

FIG. 10. Prestack depth-migrated images at the target zone for a line from the 1992 vintage, using decoupled (a) and coupled (b) velocity models.

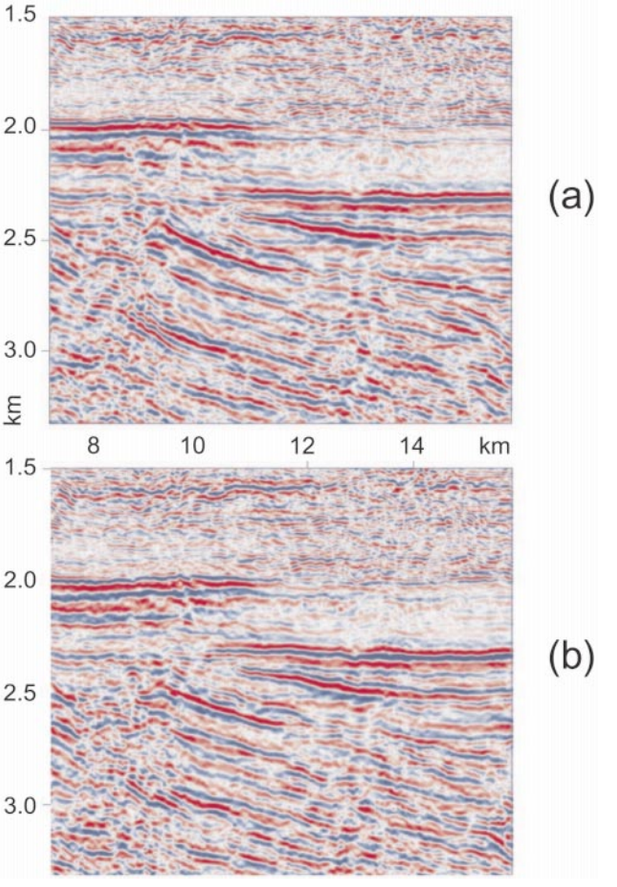

FIG. 11. Prestack depth-migrated images at the target zone for a line from the 1989 vintage, using decoupled (a) and coupled (b) velocity models.

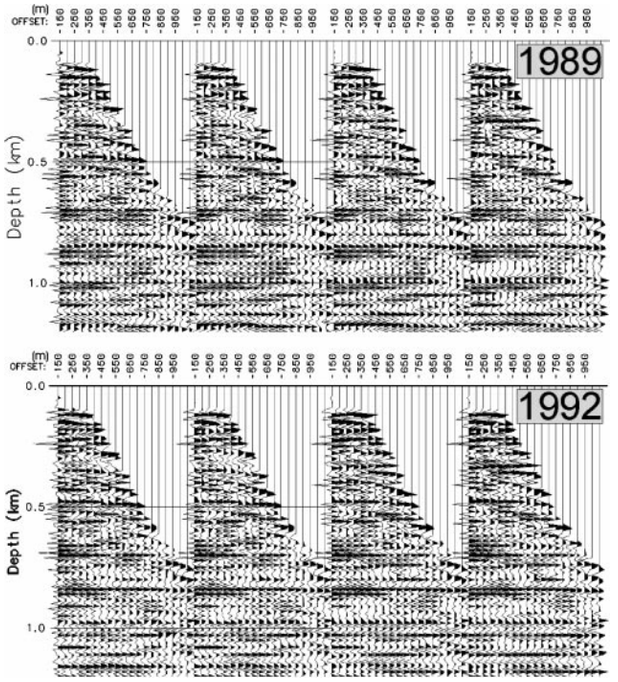

FIG. 12. Common image gathers from 1992 data, migrated using the velocities of the decoupled 1989 (top) and 1992 (bottom) model. Both gathers are flattened, but the 1992 model produces higher frequency signals.

Norsk Hydro for providing the data and for the publication permission. We thank also Stefano Picotti and Marco Peronio for their technical contributions, and Gael Janex, Alfredo Mazzotti, Eusebio Stucchi, and Paul Williamson for fruitful discussions. For the depth imaging, we used Seismic Unix from the Colorado School of Mines. A special thanks is for Rodney Calvert and Martin Landrø, who reviewed our work very carefully and constructively.

REFERENCES

Böhm, G., Rossi, G., and Vesnaver, A., 1999, Minimum time ray tracing for 3D irregular grids: J. Seis. Expl., **8**, 117–131.

Chiu, C.-S., Miller, J. H., and Lynch, J. F., 1996, Forward coupled-mode propagation modeling for coastal acoustic tomography: J. Acoust. Soc. Am., **99**, 793–802.

Davis, T., and Benson, R., 2001, Monitoring production processes by 4-D multicomponent seismic surveys at Vacuum field, New Mexico: 71st Ann. Internat. Mtg, Soc. Expl. Geophys., Expanded Abstracts, 1616–1618.

Davis, T. L., Benson, R. D., Roche, S. L., and Talley, D., 1997, 4-D, 3-C seismology and dynamic reservoir characterization—A geophysical renaissance: 67th Ann. Internat. Mtg, Soc. Expl. Geophys., Expanded Abstracts, 880–882.

Ebrom, D., Krail, P., Ridyard, D., and Scott, L., 1998, 4-C/4-D at Teal South: The Leading Edge, **17**, 1450–1453.

Johnstad, S. E., Seymour, R. H., and Smith, P. J., 1995, Seismic reservoir monitoring over the Oseberg field during the period 1989-1992: First Break, 13, 169–183.

Johnston, D. H., Eastwood, J. E., Shyeh, J. J., Vauthrin, R., Khan, M., and Stanley, L. R., 2000, Using legacy seismic data in an integrated time-lapse study: Lena field, Gulf of Mexico: The Leading Edge, **19**, 294–302.

Landrø, M., 1999, Repeatability issues of 3-D VSP data: Geophysics, **64**, 1673–1679.

——— 2001: The Gullfaks 4D seismic study: Geophysics, **66**, 836–844.

Landrø, M., Solheim, O. A., Hilde, E., Ekren, B. O., and Strønen, L. K., 1999: The Gullfaks 4D seismic study: Petr. Geosci., **5**, 213–226.

Lumley, D., Nur, A., Strandenes, S., Dvorkin, J., and Packwood, J., 1994, Seismic monitoring of oil production: A feasibility study: 64th Ann. Internat. Mtg, Soc. Expl. Geophys., Expanded Abstracts, 319–322.

Marshall, R., 1999, 4D seismics—Principles and applications: J. Seis. Expl., **8**, 309–346.

Mackenzie, K. V., 1981, Nine-term equation for sound speed in the Oceans: J. Acous. Soc. Am., **70**, 807–812.

Majer, E. L., Davis, T. L., Benson, R. D., Li, G., Coates, R. T., Korneev, V. A., and Walter, L. A., 2001, Integration of high-resolution borehole seismic data with multi-component 3D surface seismic data for cost effective reservoir recovery: 63rd Mtg., Eur. Assn. Expl. Geophys., F-24.

Nur, A., 1989, Four-dimensional seismology and (true) direct detection of hydrocarbons: The petrophysical basis: The Leading Edge, **8**, 30–36.

Rached, G., and Marshall, R., 1999, Time-lapse seismic in the Sabiryah oilfield, Kuwait: J. Seis. Expl., **8**, 383–402.

Reid, F., and MacBeth, C., 2000, Tests of vector fidelity in permanently installed multi-component sensors: 70th Ann. Internat. Mtg, Soc. Expl. Geophys., Expanded Abstracts, 1213–1216.

Rickett, J., and Lumley, D. E., 1998, A cross-equalization processing flow for the off-the-shelf 4D seismic data: 68th Ann. Internat. Mtg., Soc. Expl. Geophys., Expanded Abstracts, 16–19.

Ronen, S., Keggin, J., and van Waard, R., 1999, Repeatability of seabed multi-component data: 69th Ann. Internat. Mtg, Soc. Expl. Geophys., Expanded Abstracts, 1695–1698.

Ross, C. P., Cunningham, G. B., and Weber, D. P., 1996, Inside the cross-equalization black box: The Leading Edge, **15**, 1233–1240.

Sønneland, L., Hansen, J. O., Hutton, G., Nickel, M., Reymond, B., Signer, C. J., Tjostheim, B., and Veire, H. H., 1998, Reservoir characterization using 4-C seismic and calibrated 3-D AVO: 68th Ann. Internat. Mtg, Soc. Expl. Geophys., Expanded Abstracts, 932–935.

Sønneland, L., Veire, H. H., Raymond, B., Signer, C., Pedersen, L., Ryan, S., and Sayers, C., 1997, Seismic reservoir monitoring on Gullfaks: The Leading Edge, **16**, 1247–1252.

Stucchi, E., Mazzotti, A., and Terenghi, P., 2001, Time-lapse amplitude variations on seismic data from the Oseberg Field: 63rd Mtg, Eur. Assn. Expl. Geophys., Session P668.

Tura, A., and Lumley, D. E., 1999, Estimating pressure and saturation changes from time-lapse AVO data: 69th Ann. Internat. Mtg., Soc. Expl. Geophys., Expanded Abstracts, 16–19.

van der Sluis, A., and van der Vorst, H. A., 1987, Numerical solution of large, sparse linear algebraic systems arising from tomographic problems, *in* Nolet, G., Ed., Seismic tomography with applications in global seismology and exploration geophysics: D. Reidel Publ. Co.

Vesnaver, A., 1996, Irregular grids in seismic tomography and minimum time ray tracing: Geophys. J. Internat., **125**, 147–165.

Vesnaver, A., and Böhm, G., 2000, Staggered or adapted grids for seismic tomography?: The Leading Edge, **19**, 944–950.

Vesnaver, A., Böhm, G., Madrussani, G., Petersen, S., and Rossi, G., 1999, Tomographic imaging by reflected and refracted arrivals at the North Sea: Geophysics, **64**, 1852–1862.

Vesnaver, A., Janex, G., Madrussani, G., Mazzotti, A., Pajchel, J., Stucchi, E., and Williamson, P., 2001, Target-oriented time-lapse analysis by AVO and tomographic inversion: 71st Ann. Internat. Mtg: Soc. Expl. Geophys., Expanded Abstracts, 730–733.

Watts, G. F. T., Jizba, D., Gawith, D. E., and Gutteridge, P., 1996, Reservoir monitoring of the Magnus field through time-lapse seismic analysis: Pet. Geosci., **2**, 361–372.